Mask induced polarization effects at high NA

Andrew Estroff, Yongfa Fan, Anatoly Bourov, Bruce Smith
Rochester Institute of Technology, Microelectronic Engineering,
Rochester, NY 14623

Philippe Foubert, L.H.A. Leunissen, Vicky Philipsen
IMEC, Kapeldreef 75, B-3001 Leuven, Belgium

Yuri Aksenov
Philips Research Leuven, Kapeldreef 75, B-3001 Leuven, Belgium

ABSTRACT

It is important to understand how a photomask will polarize incident radiation. This paper presents data collected on binary mask and various attenuated phase shifting mask materials, feature sizes, duty ratios, and illumination schemes via rigorous coupled wave analysis, extinction spectroscopy, and 193nm lithographic evaluation. Additionally, the result of polarization effects due to the photomask on imaging has been studied. It was found that in the majority of the cases, higher NA led to greater polarization effects. All mask materials predominantly pass the TM polarization state for the 0 order, whereas different materials and duty ratios affect the polarization of the first diffracted orders differently. The polarization effects contributed by mask materials being considered for use in high NA imaging systems need to be examined. The degree of polarization as a function of *n* and *k* is presented, providing an introduction to the desirable properties of future mask materials. Materials with higher refractive indices and lower extinction coefficients tend to pass more of the TM polarization state, which is undesirable. Materials with lower indices and relatively wide range of extinction coefficients pass more TE polarized radiation. The duty ratio, critical dimension, mask material, material thickness, and illumination scheme all influence mask induced polarization effects.

Keywords: Photomask, Polarization, Immersion Lithography, High NA, Wire-Grid Polarizer.

1. INTRODUCTION

Polarization effects at the photomask become a concern with decreasing device dimensions and increasing NA. Minimum pitch values (Λ) on a photomask approach

$$\Lambda_{mask} = \frac{\lambda \cdot M}{(\sigma + 1) \cdot NA} \tag{1}$$

for a system with $M = 1/m$, where m is the magnification of the lens. Assuming m=0.25 (M=4 for a 4x reduction system), NA=0.85, and σ = 1.0 for current generation tools, Λ_{mask}=2.35λ (454nm at λ=193nm, ~110nm at the image plane). Next generation tools moving towards NA=1.2 will result in a minimum mask period of 1.67λ (322nm at λ=193nm, ~80nm at the image plane), at which point polarization effects contributed by the photomask are more significant.

2. HIGH NA IMAGING AND POLARIZATION

If TE polarization is defined as polarization perpendicular to the plane of incidence (POI), then radiation polarized in the POI is referred to as TM polarized (Figure 1). The angle of incidence at the wafer's surface becomes more oblique with increasing NA. For TE polarization NA is not a concern since there is no decrease in image contrast due to increased angle of incidence (θ). Image contrast, defined as the difference between the maximum and minimum intensity divided by their sum, remains 1, as shown by Equations 2[1] and 4, where δ is the phase difference (assumed to be zero). However, for TM polarization, as the angle of incidence approaches forty-five degrees, the image contrast decreases until it reaches zero at

an angle of forty-five degrees, or ninety degrees between two interfering beams (Equations 3 and 4).[1] Also, TE and TM polarized radiation states do not interfere with one another. This clearly highlights the importance of incorporating polarization into lithography modeling and simulation.

$$I_{TE} = 2|E_1|^2 (1+\cos\delta) \quad (2)$$

$$I_{TM} = 2|E_1|^2 \cdot \left[1+(\cos\delta)(\cos 2\theta)\right] \quad (3)$$

$$Contrast = \frac{I_{TE} - I_{TM}}{I_{TE} + I_{TM}} \quad (4)$$

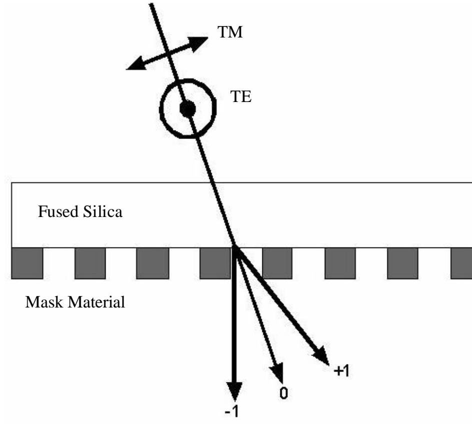

Figure 1. Unpolarized light incident upon photomask.

Traditional wire grid polarizers allow the attenuation of the TE polarized radiation while allowing the TM state to pass. The electric field of the TE polarized light induces a current in the length of the wires. Forward transmitted radiation is out of phase with the incident TE wave and exhibits greatly reduced intensity. The electric field of the TM polarized light is perpendicular to the wires, a dimension in which the wires are very narrow and restrict the motion of the electrons. Therefore, most of the TM radiation is transmitted unaffected. The parameters impacting the efficiency of a traditional wire grid polarizer include period, duty cycle, thickness, shape, and material; Johnson explains the impact of these features using Rigorous Coupled Wave Analysis (RCWA).[2] The grating period is the most important of these parameters as it determines the minimum wavelength that can be polarized for a specific diffracted order, as shown in Equation 5.

The transition region of a wire grid polarizer is defined as being between half to twice the wavelength of the incident radiation. Wood noticed a sharp decrease in transmission in this region in 1902; this phenomenon became known as Wood's Anomalies.[3] In 1907, Lord Rayleigh analyzed Wood's data and noted that for a specific wavelength (λ), period (Λ), material refractive index (n), and angle of incidence (θ), a higher diffracted order (m) emerges, as [4]:

$$\lambda = \frac{\Lambda \cdot (n \pm \sin\theta)}{m} \quad (5)$$

For feature sizes greater than twice the wavelength, a diffraction grating results with little to no polarization effects. For feature sizes less than half of the wavelength, the mask acts as a zero order wire grid polarizer. In the transition region, the mask polarizes and diffracts the radiation, and certain materials are capable of transmitting more TE polarization than TM. Wire grid polarizers passing predominantly TE polarization are appropriately named inverse wire grid polarizers, and have been studied by Honkanen et al.[5]

Traditional wire grid polarizer features are relatively large and are similar in size to the wavelength of light incident upon the polarizer; the wires approximate a planar metal surface. Inverse wire grid polarizers utilize effects similar to those that occur in "small" noble metal (Au, Ag, Cr, etc) clusters. These clusters

can be classified by their size. Feature sizes being studied in this experiment would be classified as large clusters, which experience extrinsic size effects such as collective electronic or lattice excitations known as Mie resonances. At a particular frequency (or wavelength), conduction electrons oscillate and induce polarization charges at the cluster surface, and a strong resonance is observed; this is known as a particle plasmon, and is capable of absorbing, scattering, or re-emitting the incident radiation. The conduction electrons act as an oscillatory system in clusters, but not in bulk. Sufficiently small mask features can be approximated as clusters in the small dimension (width), and as a bulk material in the long dimension (length). Therefore, TE polarized light sees a quasi-infinitely long structure, thus it looks like bulk material, and TM polarized light sees a small cluster, and induces a particle plasmon oscillation.[6,7]

3. EXPERIMENTAL SETUP

Two types of photomasks were examined: a binary mask and attenuated phase shifting masks (APSM). The polarization effects of the binary photomask were simulated using RCWA and then compared to experimentally obtained results using a Sopra variable angle spectroscopic ellipsometer (PUV-SE5). Once this data was analyzed, and RCWA was shown to be an acceptable means for measuring photomask induced polarization, APSM materials were simulated using RCWA.

The optical properties of the binary mask material used are shown in Table 1.

Layer	n	k	Thickness (nm)
Bottom (borders quartz)	1.477	1.762	73
Top (borders air)	1.939	0.941	30

Table 1. Binary mask composition.

Attenuated Phase Shifting Mask (APSM) materials were also modeled. APSM materials chosen were Tantalum Nitride in a Silicon Nitride host (TaN-Si_3N_4), Molybdenum Oxide in a Silicon Dioxide host (MoO_3-SiO_2), and Silicon in a Silicon Nitride host (Si-Si_3N_4). These materials were modeled using an effective media approximation from data collected on materials deposited via magnetron sputtering and characterized by means of ultra-violet variable angle spectroscopy (UV-VASE).[8] All masking films were designed for a π-phase shift and 10% transmission. Tables 2 and 3 contain the APSM material data.

% Composition (Host material in ***bold and italics)***					
TaN-Si3N4		**Si-Si3N4**		**MoO3-SiO2**	
TaN	***Si3N4***	Si	***Si3N4***	MoO3	***SiO2***
17.0%	83.0%	9.0%	91.0%	30.0%	70.0%

Table 2. APSM material composition.

	TaN-Si3N4	Si-Si3N4	MoO3-SiO2
n	2.5626	2.4317	1.5891
k	0.489	0.4462	0.2117
Thickness (A)	631	687	1647
% Transmission	9.88	10.4	9.69

Table 3. APSM material data.

GSolver was used to perform the simulations in this experiment.[9] GSolver is a visual grating structure editor utilizing full 3-dimensional vector code using hybrid RCWA and modal analysis and is capable of analyzing arbitrary grating thickness, number of materials, and material index of refraction. Additionally, it is capable of modeling multiple materials, buried structures, and varied shapes (represented by stacked layers).

Unpolarized radiation was simulated by inputting a 100% TE polarized beam and measuring the transmitted TE intensity in the 0th and 1st diffracted orders and then doing the same for a 100% TM polarized beam. This was done for 193nm radiation for both normal and off-axis illumination, where off

axis illumination was defined for this experiment as having an NA=1.2, which corresponds to 17.45 degrees in air, or 11.08 degrees in quartz (n=1.56 at λ=193nm). The mask pitch was varied from 0nm to 1000nm, and for the binary mask duty ratios examined were 0.2, 0.25, 0.33, and 0.5. Degree of Polarization (defined here in Equation 6) was plotted versus mask pitch for the different materials, feature shapes, duty cycles, and wavelengths.

$$DoP = \frac{T_{TE} - T_{TM}}{T_{TE} + T_{TM}} \tag{6}$$

By this definition, a degree of polarization of –1 signifies fully TM polarized radiation, +1 signifies fully TE polarization, and 0 represents equal TE and TM polarization.

The binary mask extinction spectroscopy measurements were performed on a Sopra tool, shown in Figure 2. Similar to the simulations, 100% TE polarized incident radiation illuminated the mask and the transmitted radiation was measured; this was repeated for 100% TM polarized radiation. All measurements were made with 193nm radiation. This was performed for a duty ratio of 0.5 and for mask pitches of 250nm, 300nm, 350nm, 500nm, 600nm, and 800nm. Due to tool limitations, for normal incidence only the 0th and -1st orders could be measured, and only the -1st order could be measured for off-axis illumination. DoP (as defined by Equation 6) was plotted vs. mask pitch and compared to simulated results.

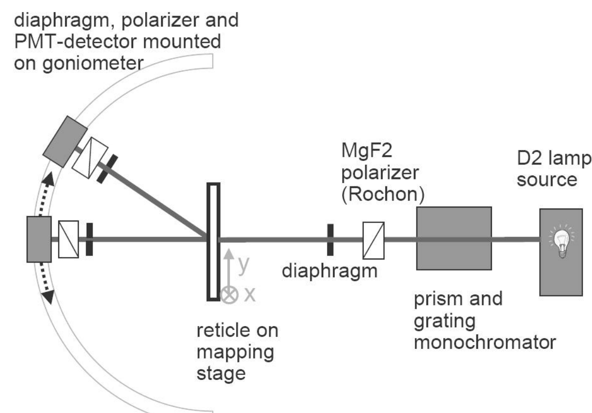

Figure 2. Schematic of Sopra tool.

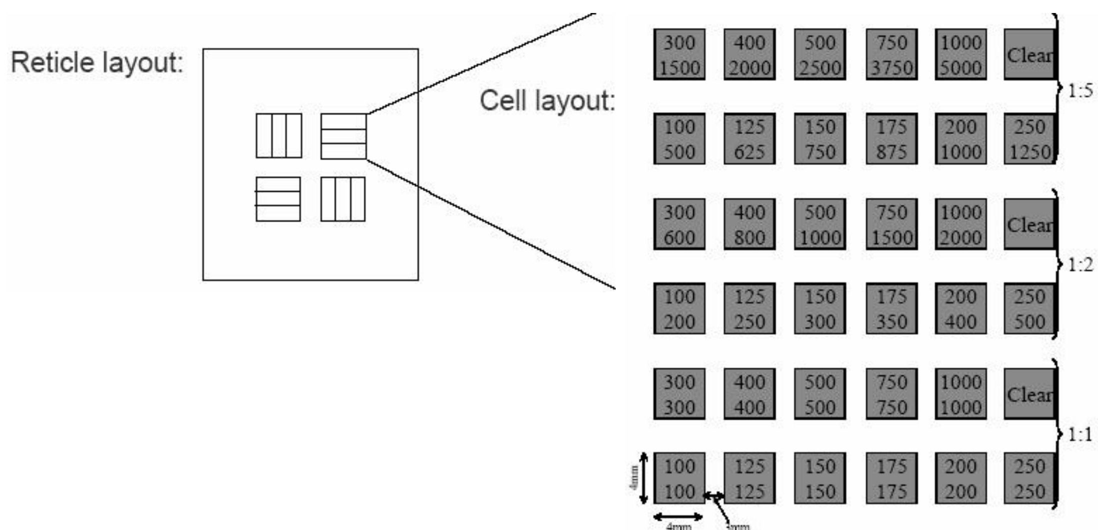

Figure 3. Schematic of the reticle used in this experiment.

4. RESULTS

The Wood's Anomaly equation can be rearranged to provide the grating pitch at which a particular order emerges. For all on axis cases in this experiment, this corresponds to the first order emerging at $\Lambda=\lambda$. At this point, the 0-order in all cases experiences a decrease in transmission, and usually is also the mask pitch at which the 0-order experiences the greatest polarization effects.

The diffraction spectra measured by the Sopra tool for a few of the measured cases is shown in Figure 4 A-D. It is observed for the smaller mask pitches that the first order is hard to measure due to the background noise (spectrum shown in Figure 5A). To resolve this problem, a scan was done for the smaller pitches (250nm, 300nm, 350nm), and the results for the 125nm case are shown in Figure 5-B; this is a much cleaner signal. In the calculation of the DoP for these smaller pitches, the averaged background noise was subtracted from the 1st order signal.

Observed in Figure 4-B is a double peak in the 1st order measurement; this area is expanded in Figure 5-C. This is believed to be caused by the excitation of multipolar plasmons, which can result in a broadening of the transmission peak.[6,7]

A "half-order" anomaly is observed in Figure 4-A, B, D (and is present in all cases measured except for pitch = 500nm, Figure 4-C). A closer look at this phenomenon is shown in Figure 5-D. This anomaly experiences a shift in both peak position and size depending upon the mask pitch. For measured pitches below 500nm it appears at approximately 70% of the distance between the 0th and 1st orders and has higher peak intensity than the 1st order, and for measured pitches larger than 500nm it is smaller in magnitude than the 1st order and appears at an angle of about 50% between the 0th and 1st orders.

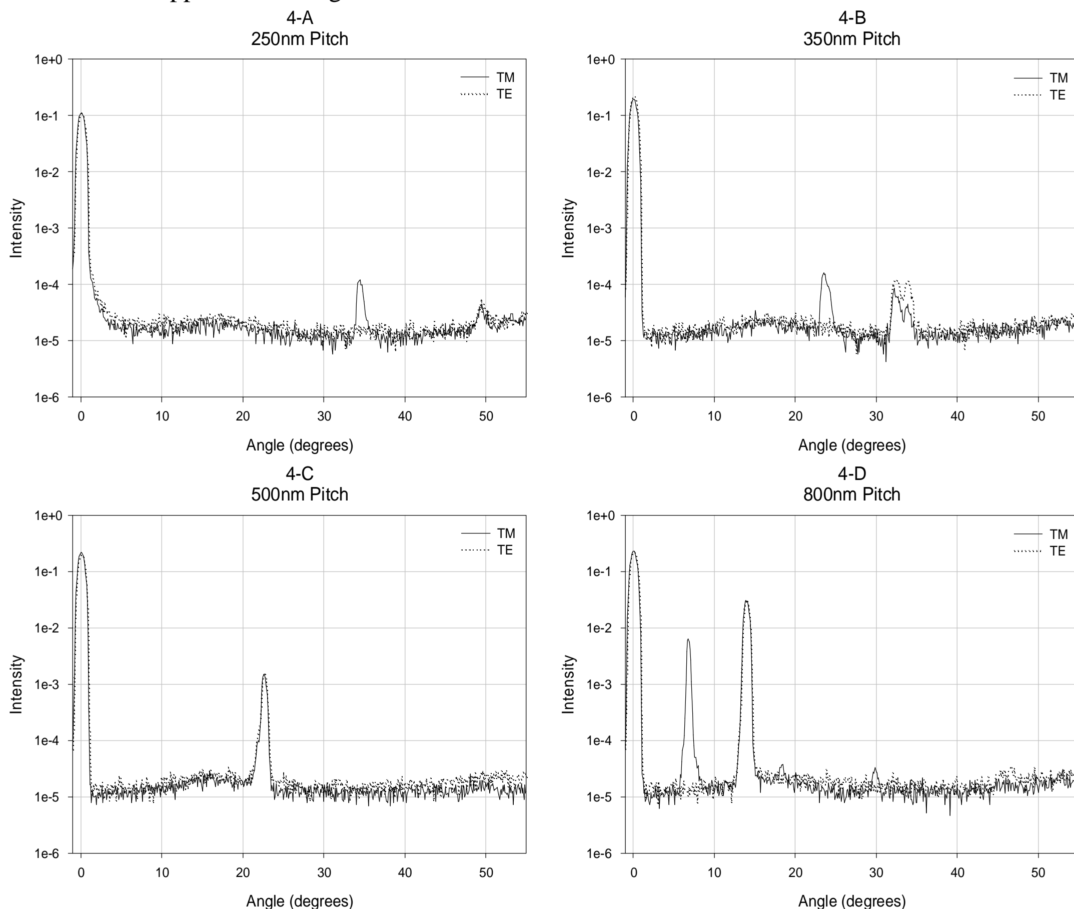

Figure 4 A-D. Diffraction Spectra of A) 250nm Pitch, B) 350nm Pitch, C) 500nm Pitch, D) 800nm Pitch. Note absence of half-order in 500nm pitch case, and presence of double peak in the 1st order of the 175nm pitch case.

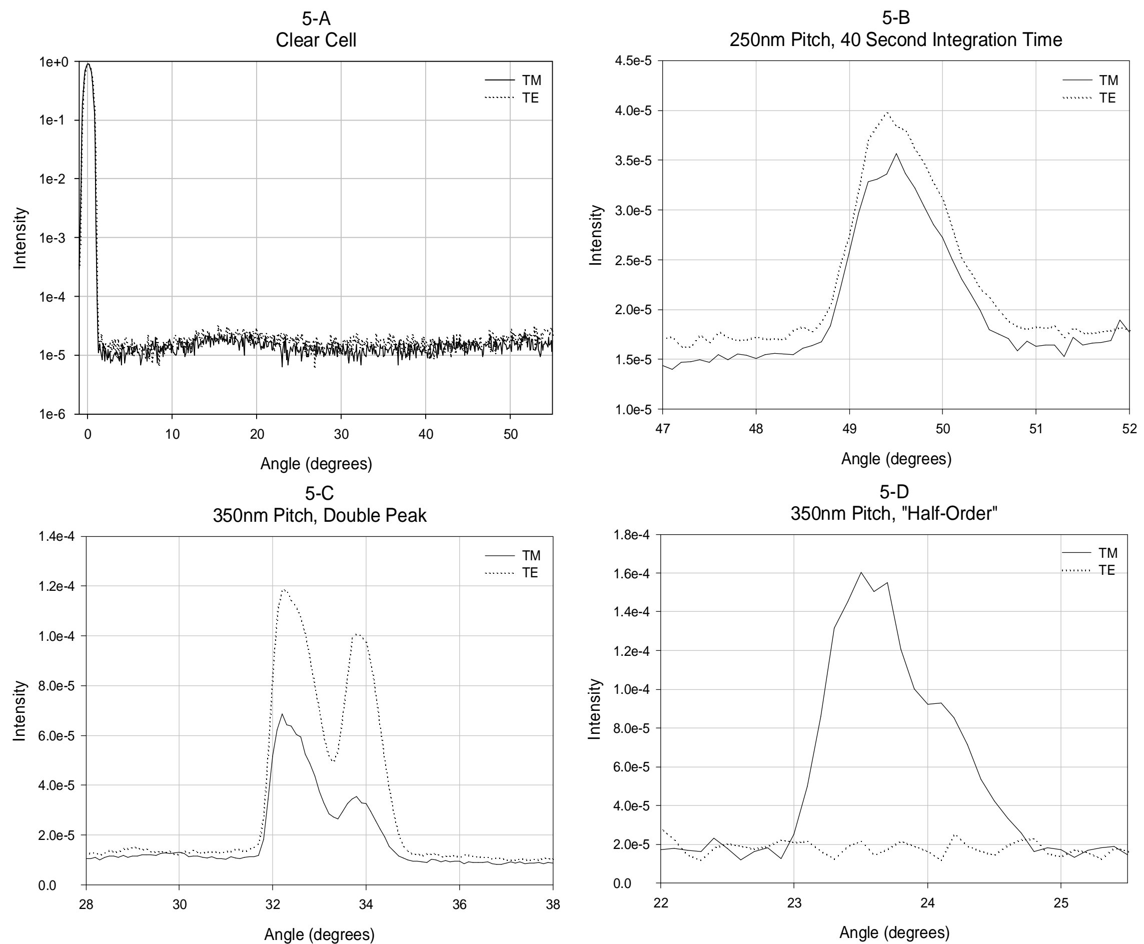

Figure 5 A-D. Diffraction spectra of A) clear cell on mask, B) 1st Order for 250nm pitch measured with a 400second integration time, C) double peak observed in 350nm pitch case, D) TM polarized half-order observed in 350nm pitch case.

This half-order anomaly is only visible for TM polarization. It is possible that the incident TM polarization for the pitches where this is present is exciting a surface plasmon, which could be re-emitting at the angle corresponding to this anomaly. Although there seem to be several theoretical explanations accounting for the occurrence of the double peak and the "half-order", these anomalies need to be investigated further.

After measuring the diffraction spectra for the mask pitches mentioned previously, the DoP was calculated for the 0th and -1st orders for normal incidence, and for the -1st order for off-axis illumination. The results for the binary mask are shown in Figure 6 A-D.

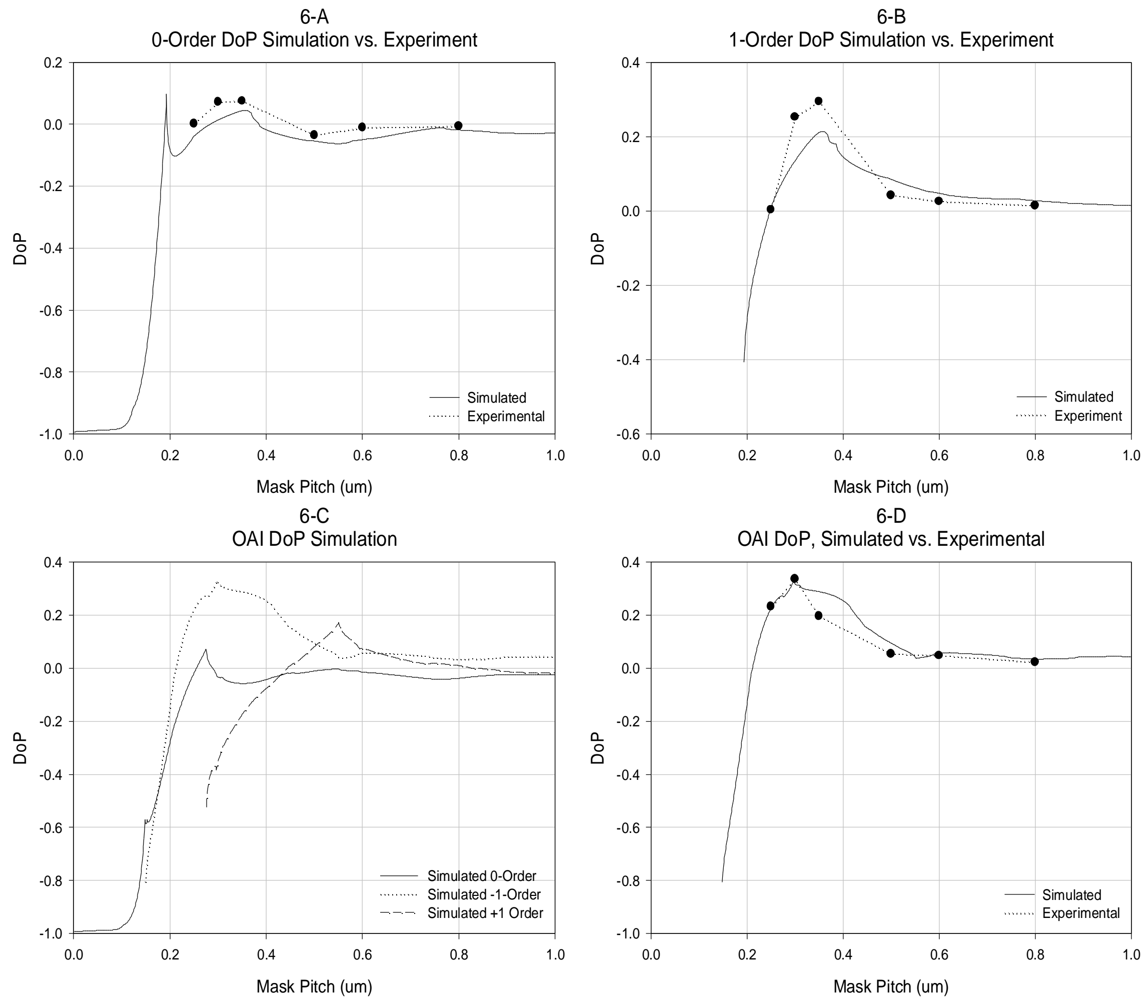

Figure 6 A-D. Binary mask DoP vs. Mask Pitch for A) 0-Order normal incidence, B) 1-Order normal incidence, C) OAI simulation only, D) -1-Order, OAI simulation vs experiment.

Figure 6 shows that RCWA provides results similar to those obtained experimentally. Discrepancies between experiment and simulation can partly be attributed to inaccurate n and k values used for the mask. Additionally, the actual mask pitch and fill factor/duty ratio has not been measured yet; these were assumed to be exactly as designed.

For the 0th order, the binary mask acts as a strong TM polarizer for mask pitches less than the illuminating wavelength, but as a weak polarizer at greater pitches. For the 1st order the binary mask acts as a strong TM polarizer where the 1st order initially emerges, as a relatively strong TE polarizer throughout most of the transition region, and as a weak TE polarizer at pitches greater than 2λ. For OAI, the 0th order is polarized similarly as it is in the normal incidence case, but the -1st order is polarized more strongly than in the normal incidence case, and emerges at a smaller mask pitch. The $+1^{st}$ order emerges at a larger mask pitch, and experiences slightly decreased polarization effects.

Noticing that RCWA provides similar results to those obtained experimentally, more simulations were performed. Figure 7 shows simulated results for the binary mask with normally incident illumination and differing duty ratios. It is observed that smaller duty ratios generally decrease polarization effects for a given critical dimension (CD).

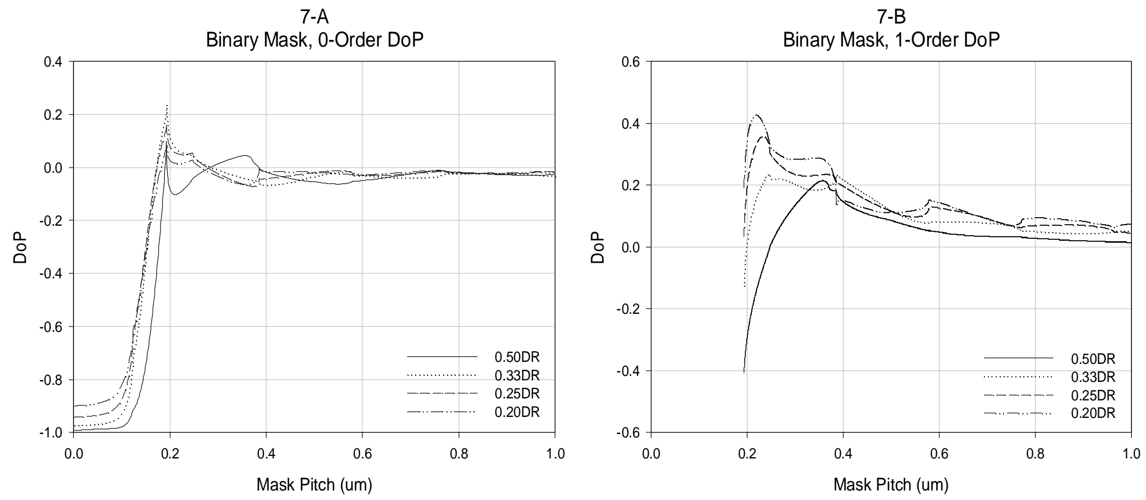

Figure 7-A,B. On axis illumination of the binary mask for differing duty ratios.

Simulations were also performed for the APSM materials shown in the experimental setup (note that due to the similar optical properties of TaN-Si_3N_4 and Si-Si_3N_4 that only the TaN-Si_3N_4 results are shown here for brevity). The results for on and off-axis illumination are shown in Figure 8 A-D. For on-axis illumination in general the APSM materials act as strong TM polarizer for the 0th order for mask pitches within the transition region as well as mask pitches greater than 2λ. The 1st order is strongly TM polarized within the transition region, but acts as a weak polarizer for larger pitches. The trends for off-axis illumination follow those observed in the binary mask case. Typically, thicker films polarize more strongly than thinner films, however, the metallic oxides (thicker) polarize less strongly than the metallic nitrides (thinner); thickness as a function of *n* and *k* is shown in Figure 9. Since thinner materials are desired for future technology nodes, this is a potentially unfavorable interaction.

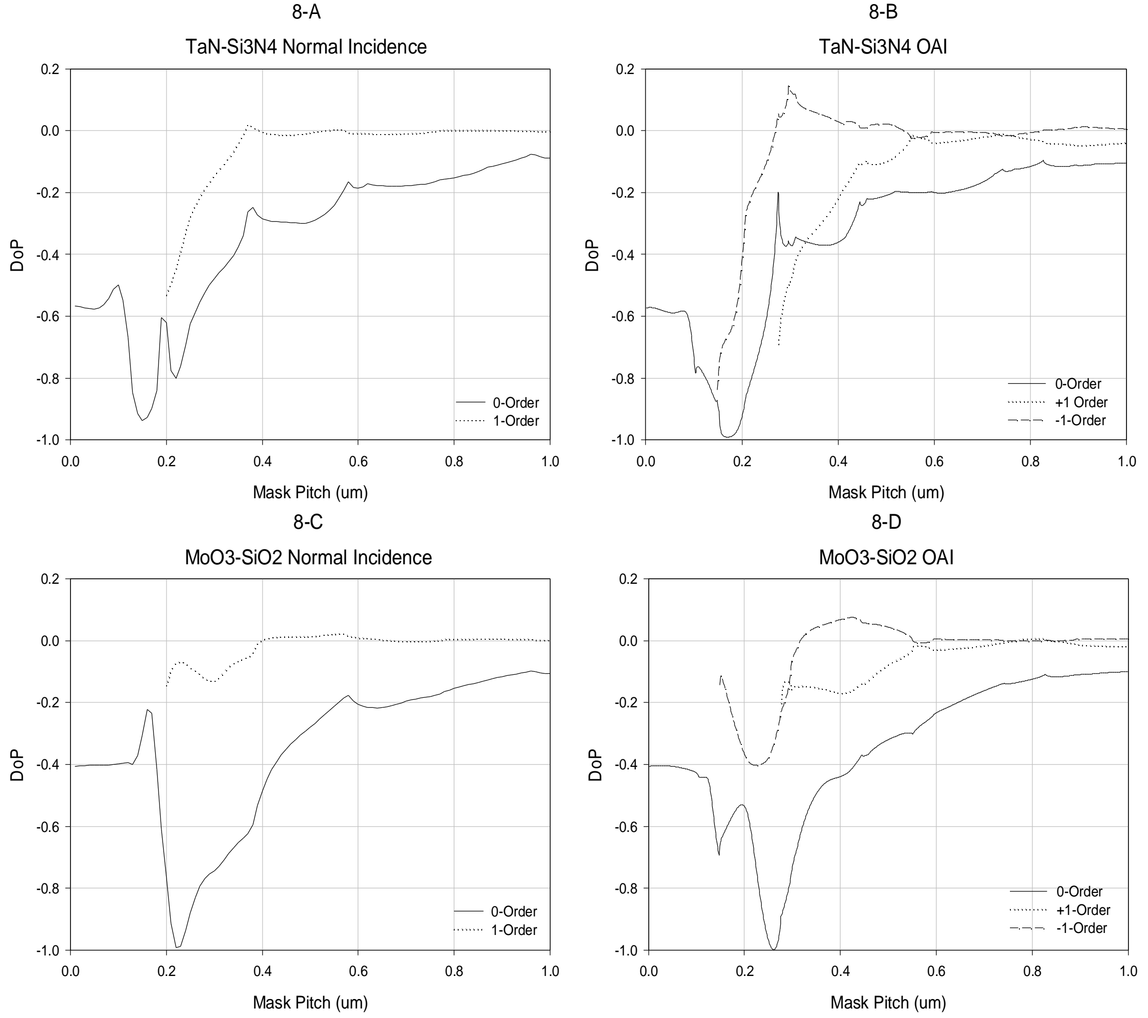

Figure 8 A-D. On and Off-axis illumination for different APSM films.

Noticing that APSM materials predominantly pass the TM state of polarization, which provides relatively poor imaging, it is necessary to look at other possible materials. Additional simulations were performed to study the degree of polarization as a function of n and k for π-phase shifting APSM materials. The index of refraction was varied from 0.5 to 3.0 (increments of 0.1) and the extinction coefficient from 0.0 to 1.0 (increments of 0.1). The thickness necessary to obtain a π-phase shift was calculated for a particular n and k value by first using Equation 7 to calculate the interfacial phase jump at the substrate-mask material interface ($\Delta\Phi_{12}$), the mask material-air interface ($\Delta\Phi_{23}$), and the substrate-air interface ($\Delta\Phi_{13}$), and using these values in Equation 8 to solve for d.[11] A plot of APSM film thickness vs. n and k is shown in Figure 9. This thickness, d, was then used to calculate transmission as a function of n and k using Equation 9.[11, 12] An extinction coefficient was found for a particular transmission and index of refraction, and lines were superimposed on the contour plot for 4% and 15% transmission. Shown in Figure 10 is the contour plot of degree of polarization vs. n and k with transmission lines overlaid.[13] The DoP was calculated for the limit of a 1.2NA system described previously (~40nm half pitch on wafer).

$$\Delta\Phi_{12} = \arg\left(\frac{2n_1^*}{n_1^* + n_2^*}\right) \quad (7)$$

$$\Delta\Phi = \frac{2\pi}{\lambda}(n_2 - n_3)d + \Delta\Phi_{12} + \Delta\Phi_{23} - \Delta\Phi_{13} \quad (8)$$

$$T(k) = \frac{(1-R_{12})\cdot(1-R_{23})}{(1-R_{13})}\cdot e^{\frac{-4\pi}{\lambda}k\cdot d} \tag{9}$$

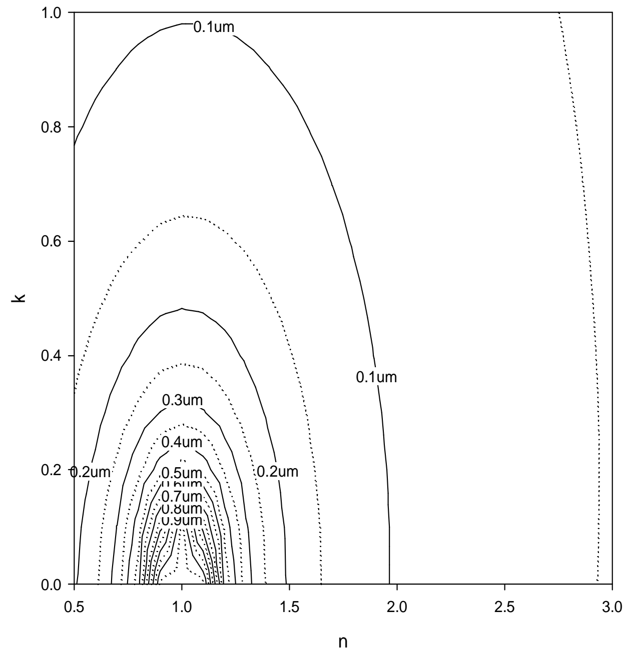

Figure 9. APSM material thickness vs. n and k.

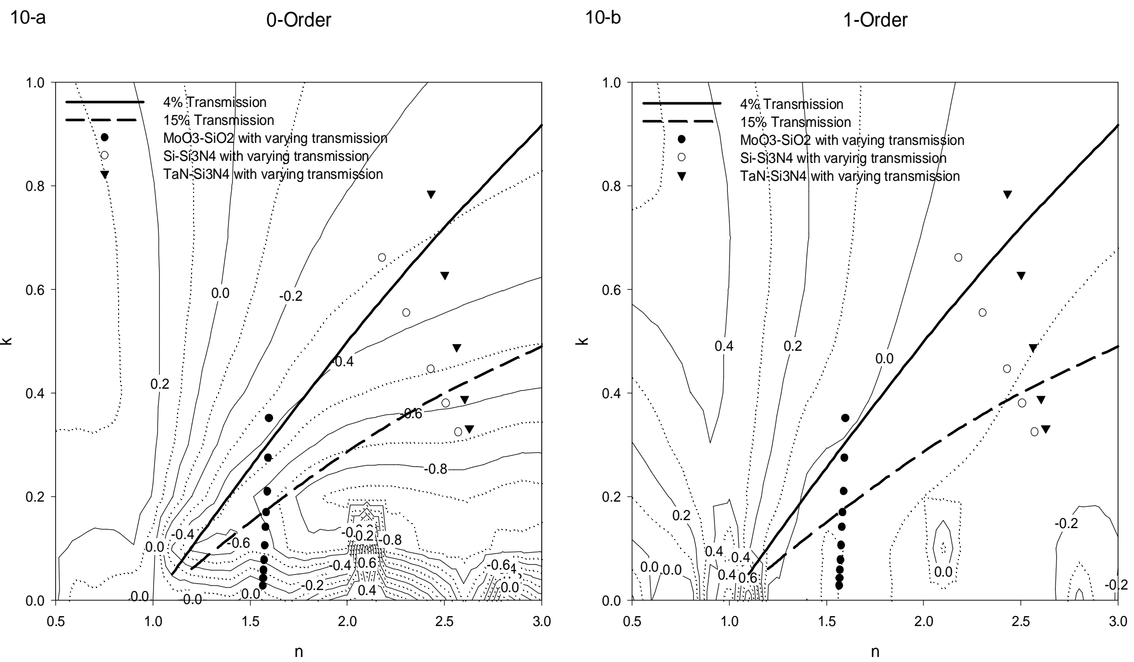

Figure 10. DoP as a function of n and k for π-phase shifting materials

It is observed that materials with higher refractive indices and lower extinction coefficients tend to pass more of the TM polarization state. Materials with lower refractive indices and a relatively wider range of extinction coefficients pass more TE polarized radiation. Higher refractive index films are thinner than those with lower refractive indices.

Additionally, the APSM materials with transmission varying from 2-20% (2-70% for MoO3-SiO2) were superimposed on the contour plot to show viable candidates for next generation mask materials. Materials that contribute more TE polarization effects or equal polarization weighting are desirable. From Figure 10, materials that meet these criteria with a transmission between 4-15% have an index of refraction between 1.1 and 1.4, and an extinction coefficient between 0.05 and 0.2. None of the materials examined in this paper meet the desired polarization criteria. It should be noted, however, that although the 0th order is polarized strongly in the TM state between the overlaid transmission curves, the 1st order remains mainly unpolarized, or slightly TM polarized.

Having studied how all of these different mask materials polarize radiation, it would be useful to know how this affects imaging. A kirchoff mask (2-D, no polarization effects) was simulated in Solid-CM for half pitch values of 45nm, 65nm, and 90nm (corresponding to mask pitches of 360nm, 520nm, and 720nm) with off-axis illumination of NA=1.2.[14] The DoP values for the 0th and -1st orders for the binary and TaN-Si_3N_4 were applied as pupil-polarization filters at the proper position where the orders would be passing through the pupil. By doing this, the impact of polarization only on imaging can be observed. The contrast improvement due to mask polarization is shown in Figure 11.

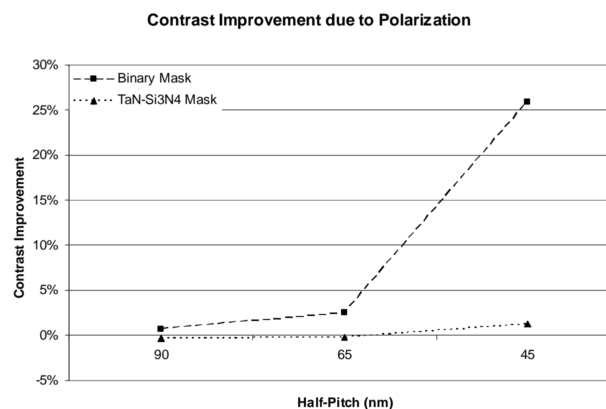

Figure 11. Contrast improvement due to polarization.

Although the 0th order is relatively strongly polarized in the TM state for the APSM mask, the 1st order is weakly polarized, and thus there is little change in contrast due to polarization. A greater than 25% increase in contrast is observed in the binary mask due to the predominantly TE polarized 1st order. The polarization of the 0th order does not seem to have a large impact on contrast.

5. CONCLUSIONS

Rigorous coupled wave analysis was verified with complimentary experiments as a useful tool in studying photomask induced polarization effects. Material constants and thickness, as well as feature size and shape need to be known accurately to obtain the best results. Experiments were performed on a binary mask for various mask pitches and illumination conditions. More experiments need to be performed to further study the anomalies seen in the diffraction spectrum of the binary mask. Additional simulations were performed for various mask pitches, duty ratios, material thicknesses, mask materials, and illumination schemes. Image contrast improvement due to polarization was also examined.

It was observed that mask polarization effects depend on most any factor that can be changed: illumination, mask material, material thickness, mask pitch, and duty ratio. In all cases, higher NA (or smaller critical dimensions) results in greater polarization effects. A smaller duty ratio for a given CD usually results in a

decrease in polarization effects. Off-axis illumination allows for greater polarization effects in the 1st diffracted order emerging at a smaller mask pitch.

For the 0th order, binary photomasks were found to act as strong TM polarizers for sub-wavelength features, and very weak polarizers after the 1st order emerge. They polarize the 1st order predominantly TE in the transition region of wire-grid polarizers, and do not polarize much outside of this region.

APSM photomasks were found to strongly polarize the 0th order in the TM state for all mask pitches examined, the 1st orders were mainly polarized in the TM state as well, but this is confined mostly to mask pitches in the transition region. There do exist n and k combinations for π-phase shifting materials that pass more TE polarization or contribute no polarization weighting, however, they may not be practical.

Image contrast can be improved due to slightly more TE than TM polarization in the 1st order, whereas the polarization of the 0th order does not seem to have much of an effect on image contrast at all. APSM materials, although predominantly TM polarizing, do not seem to have much effect on image contrast at the technology nodes examined. At these nodes, the 1st order is very weakly polarized.

REFERENCES

1. D. Flagello, Vector Diffraction Analysis of Phase-Mask Imaging in Photoresist Imaging, proc. SPIE vol. 1927, p. 395-412, 1993
2. J. H. Johnson, *Wire Grid Polarizers for Visible Wavelengths*, PhD dissertation, University of Rochester, Rochester, NY, 2003
3. R. W. Wood, *Uneven Distribution of Light in a Diffraction Grating Spectrum*, Philosophical Magazine, September, 1902
4. Lord Rayleigh, *On the Remarkable Case of Diffraction Spectra Described by Prof. Wood*, Philosophical Magazine, July, 1907
5. Honkanen et al, *Inverse Metal-Stripe Polarizers*, Applied Physics B **68**, 81-85, 1999
6. Kreibig, Uwe, Optical Properties of Metal Clusters, Springer, Berlin, 1995
7. G. Schider, *Optical properties of Ag and Au nanowire gratings*, Journal of Applied Physics, October 15, 2001, Volume 90, Issue 8, pp. 3825-3830
8. Rochester Institute of Technology, Materials Database, http://www.microe.rit.edu/research/lithography/utilities.htm
9. GSolver, http://www.gsolver.com
10. Stephen Wedge, Surface plasmon-polariton mediated light emission through thin metal films, Optics Express, vol. 12, no. 6, August 9, 2004
11. B. Smith, Attenuated phase shift mask materials for 248 and 193nm lithography, J. Vac. Sci. Technol. B 146(6), Nov/Dec 1996
12. A. Bourov, *Optical properties of materials for 157nm lithography*, M.S. Thesis, RIT, Rochester, NY, 2003
13. A. Estroff, *Mask induced polarization effects at high NA*, publishing pending in JM3, initially submitted November, 2004.
14. Solid-CM, Sigma-C, http://www.sigma-c.com